Gal Repressor−Operator−HU Ternary Complex: Pathway of Repressosome Formation

Siddhartha Roy,[‡,§,||] Emilios K. Dimitriadis,[‡,⊥] Sudeshna Kar,[||] Mark Geanacopoulos,[||,#] Marc S. Lewis,[⊥] and Sankar Adhya*[,||]

Department of Biophysics, Bose Institute, Calcutta 700019, India, and Laboratory of Molecular Biology, National Cancer Institute, Bioengineering and Physical Science, ORS, OD, and Laboratory of Molecular Biology, National Heart, Lung, and Blood Institute, National Institutes of Health, Bethesda, Maryland 20892

Received October 26, 2004; Revised Manuscript Received January 26, 2005

ABSTRACT: DNA transaction reactions require formation of nucleoprotein complexes that involve multifaceted DNA−protein and protein−protein interactions. Genetic and biochemical studies suggested that the higher order Gal repressosome structure, which governs the transcription of two tandem *gal* promoters in *Escherichia coli*, involves sequence-specific binding of GalR repressor dimers to two operators, O_E and O_I, located 113 bp apart, binding of GalR to the sequence-nonspecific DNA binding protein HU, interaction of HU with an architecturally critical DNA site between the two operators, and interaction between two DNA-bound GalR dimers generating a loop of the intervening DNA segment. In this paper, we demonstrate and determine the thermodynamic parameters of several of these interactions, GalR dimer−O_E, GalR tetramerization, HU−GalR, and HU−GalR−O_E interactions, by analytical ultracentrifugation, fluorescence anisotropy, and fluorescence resonance energy transfer. The physiological significance of several of these interactions was confirmed by the finding that a mutant HU, which is unable to form the repressosome in vivo and in vitro, failed to show the HU−GalR interaction. The results help to construct a pathway of Gal repressosome assembly.

An important step in the regulation of gene expression is the initiation of transcription. In prokaryotes, a typical pattern for negative regulation appears to be binding of two repressor molecules to bipartite operators, establishment of repressor−repressor contact by looping of the intervening DNA (*1*, *2*), and inhibition of transcription initiation by the looped structure (*3*). The formation of a DNA loop in the *gal* operon of *Escherichia coli* requires binding of two GalR[1] repressor molecules to two *gal* operators, separated by 113 bp (*4*). DNA looping in *gal* also requires the binding of the DNA-bending protein HU around the middle of the looped DNA (*5*). The HU−GalR−DNA loop complex has been termed the repressosome (*6*). Whereas GalR is a homodimer of a 37 kDa subunit (*7*), HU is a small heterodimeric histone-like protein with a subunit size of 9 kDa. HU binds to DNA without any sequence specificity and with low affinity, and it binds to bent or distorted DNA with higher affinity (*8*−*12*). In the Gal repressosome, however, HU is localized in a specific region (*hbs*) of the DNA loop, possibly due to the looping-induced distortion of the DNA (*13*). Since the binding of HU to *hbs* is totally dependent upon the binding of GalR to the operators, a protein−protein interaction between GalR and HU may explain the cooperativity in DNA binding (*13*). A GalR−HU interaction was suggested by isolation and genetic and biochemical characterization of HU mutants that failed to form the *gal* DNA loop even though their ability to bind DNA was not compromised (*14*). In this paper, we report physical interactions between the different interacting partners, including GalR and HU, of the proposed repressosome complex, and determine the energetics of these interactions. By similarly characterizing a HU mutant, we confirm a physiological role of the specific GalR−HU contact in repressosome formation.

EXPERIMENTAL PROCEDURES

Materials. IAEDANS was purchased from Molecular Probes Inc. (Eugene, OR). Purified oligonucleotides were obtained from SAIC-Frederick Cancer Research Facility (Frederick, MD). The 20 bp DNA duplex of the sequence 5′TTGTGTAAACGATTCCACTA3′ (with a 5′-amino link) containing the *gal* operator O_E was used in fluorescence experiments. The 20 bp DNA duplex without the 5′-amino link and a 28 bp long duplex containing an additional 4 bp (CTTA) at the 5′ end and another 4 bp (ATTA) at the 3′ end were used in the ultracentrifugation studies. Other reagents were of analytical grade.

Protein Purification. GalR was purified according to Majumdar et al. (*15*), wild-type HU and HUαA43/β were purified according to Aki and Adhya (*13*), and the HUαK18A homodimer was purified according to Kar and Adhya (*14*).

* To whom correspondence should be addressed at the Laboratory of Molecular Biology, National Cancer Institute, 37 Convent Drive, Room 5138, Bethesda, MD 20892-4264. Tel: (301) 496-2495. Fax: (301) 402-1344. E-mail: sadhya@helix.nih.gov.

‡ Contributed equally to this work.

§ Bose Institute.

|| National Cancer Institute, NIH.

⊥ Bioengineering and Physical Science, ORS, OD.

National Heart, Lung, and Blood Institute, NIH.

[1] Abbreviations: HU, heat unstable protein; GalR, Gal repressor; O_E, external *gal* operator DNA.

10.1021/bi047720t
Published on Web 03/17/2005

Ultracentrifugation. Analytical ultracentrifugation was performed in a Beckman XL-A analytical ultracentrifuge using an eight-hole rotor at a rotor speed of 10000 rpm. Measurements were started at 2 °C and repeated in increments of 4 °C each time after ascertaining that equilibrium had been reached and/or until the samples showed clear signs of degradation. Data were collected up to the temperature of 18 °C. After each temperature change equilibrium was reached after about 24 h. Two sets of experiments were performed with the wild-type HU in the first set and the mutant HUαK18A homodimer in the second set. The buffers used in the ultracentrifugation studies were 250 mM KCl and 50 mM Tris-HCl, pH 8.0, in the first set of experiments and 75 mM KCl and 50 mM Tris-HCl, pH 8.0, in the second set. The channels in the seven sample cells were loaded with 180 μL of the following materials: cell 1, 1.95 or 1 μM GalR; cell 2, 15 μM wild-type HU or 5.8 μM HUαK18A homodimer; cell 3, 1.4 or 1.5 μM 20 bp DNA duplex; cell 4, 0.61 or 0.5 μM GalR and the corresponding equimolar amount of 28 or 20 bp DNA duplex; cell 5, 1.4 or 2.4 μM each of HU (wild type or mutant) and the corresponding equimolar amount of 28 or 20 bp DNA duplex; cell 6, 0.34 μM GalR, 0.34 μM 28 bp DNA duplex, and 0.94 μM wild-type HU (1.41 OD) or 0.32 μM GalR, 0.32 μM 20 bp DNA duplex, and 1.8 μM HUαK18A (0.31 OD); cell 7, 0.41 μM GalR, 0.41 μM 20 bp DNA duplex, and 1.875 μM HU or 0.41 μM GalR, 0.21 μM 28 or 20 bp DNA duplex, and 1.3 μM HUαK18A homodimer.

Because the speed of these runs was too low for sedimentation of the HU homodimer, we ran another wild-type HU sample of similar concentration at 24000 rpm and at 4 °C. That gave enough concentration gradient to enhance our confidence in the multiwavelength results. The second channel of each cell was filled with 185 μL of the buffer. Transmitted light intensities were collected at five different wavelengths, 230, 233, 236, 239, and 242 nm, and at radial increments of 0.001 cm. Nine replicates were collected and averaged for each data point. Data were fitted to appropriate mathematical models of sample concentration radial distributions using the weighted, least-squares algorithms of the MLAB software package (Civilized Software, Inc., Bethesda, MD) on a Pentium III-based personal computer. The problem formulation and analysis followed the multiwavelength method developed by Lewis et al. (*16*) to study the interactions between species with significantly different absorption spectra. The presence of the DNA required the multiwavelength approach because of its very strong absorption at 280 nm where the proteins were usually examined. Extinction coefficients for the two proteins at the wavelengths of interest were measured in a Pharmacia Ultrospec 3000 spectrophotometer.

Data Analysis of Ultracentrifugation Experiments. In a solution column that reaches equilibrium at temperature T, the total absorption at radius r and wavelength λ_i may be written in terms of total molar concentrations of the various monomeric protein species, $C_{n,T}$, and their corresponding extinction coefficients, $E_{n,\lambda}$

$$A_{T,\lambda_i}(r) = \sum_n E_{n,\lambda_i} C_{n,T}(r) \qquad (1)$$

where n ranges over the number of different monomer species in the solution. These equations were used to compute least-squares estimates for $C_{n,T}(r)$. The simplest model assumed a single species and was used to compute a mean molecular mass of the various species in the solution. Such estimates helped to constrain the range of association models we needed to examine. An assumed interaction model was fitted to the data to obtain the equilibrium constants for the associations. The quality of the fit indicated the consistency of the assumed model with the experimental data.

Chemical Modification. A 0.5 mL solution of HUαA43C/β was dialyzed overnight against 0.1 M potassium phosphate buffer, pH 8.0. To this solution was added 9.2 mg of solid IAEDANS, and the solution was incubated on ice and in the dark for 3 h. The solution was then extensively dialyzed against 0.1 M Tris-HCl, pH 7.5, containing 0.1 M NaCl at 4 °C. The O_E-containing 20 bp amino-linked DNA was end-labeled with fluorescein according to Bandyopadhyay et al. (*17*) and was in 0.05 M Tris-HCl, pH 8.0, 0.01 M $MgCl_2$, and 0.1 M NaCl.

Fluorescence Spectroscopy. Fluorescence anisotropy measurements were carried out in a PANVERA fluorometer fixed for automatic polarization measurements at 25 °C. The excitation filter was set at 330 nm and the emission filter around 485 nm. AEDANS−HUαA43C/β was in 0.1 M Tris-HCl, pH 7.0, containing 0.3 M NaCl.

Fluorescence resonance energy transfer experiments were carried out in a Perkin-Elmer LS50B spectrofluorometer. GalR monomer contains a single tryptophan residue. Fluorescence energy transfer experiments between GalR tryptophan and AEDANS−HUαA43C/β were conducted as follows. The oligonucleotide was annealed in 0.05 M Tris-HCl, pH 7.5, containing 0.1 M NaCl and 10 mM $MgCl_2$. The AEDANS−HUαA43C/β was dialyzed in 0.1 M Tris-HCl, pH 7.5, containing 0.1 NaCl. The GalR was dialyzed in 0.05 M Tris-HCl, pH 8.0, containing 0.6 M NaCl and 10% glycerol. Buffers and other stock solutions were mixed in proportions to create the following mixtures having the same buffer composition: (A) 7.5 μM O_E−DNA + 7.5 μM AEDANS−HUαA43C/β + 7.5 μM GalR dimer; (B) 7.5 μM O_E−DNA + 7.5 μM AEDANS−HUαA43C/β; (C) 7.5 μM O_E−DNA + 7.5 μM GalR dimer; and (D) buffer. The final buffer composition was 0.04 M Tris-HCl, pH 7.5, 0.3 M NaCl, 4% glycerol, and 1.5 mM $MgCl_2$. Excitation spectra (280−450 nm) of each of the solutions were recorded in a 0.5 cm × 0.5 cm path length cuvette with emission set at 480 nm. The spectrum of D was subtracted from that of B to obtain pure acceptor spectra (F_A). The spectrum of C was subtracted from that of A to obtain donor + acceptor spectra (F_{D+A}). F_{D+A} and F_A were compared to determine the energy transfer efficiency.

Fluorescence energy transfer between fluorescein end-labeled DNA and AEDANS−HUαA43C/β was carried out as follows. Stock solutions of annealed DNA and AEDANS−HUαA43C/β were made in 0.05 M Tris-HCl, pH 8.0, containing 10 mM $MgCl_2$ and 0.1 M NaCl. GalR was dialyzed in 0.05 M Tris-HCl, pH 8.0, containing 0.6 M NaCl and 10% glycerol. Buffers and other stock solutions were mixed in proportions to create the following mixtures having the same buffer composition: (A) 2.18 μM fluoresceinated O_E−DNA; (B) 3 μM AEDANS−HUαA43C/β + 2.18 μM fluoresceinated O_E−DNA; (C) 3 μM AEDANS−HUαA43C/β; (D) 1.75 μM GalR dimer + 3 μM AEDANS−HUαA43C/β

+ 2.18 μM fluorosceinated O_E−DNA; and (E) buffer. The final composition of the buffer was 0.05 M Tris-HCl, pH 8.0, 0.3 M NaCl, 0.4% glycerol, and 1.5 mM $MgCl_2$. Excitation spectra of each of the solutions were recorded from 300 to 525 nm with emission wavelength set at 535 nm. The spectrum of E was subtracted from that of A to obtain pure acceptor spectra (F_A). The spectrum of C (direct donor) was subtracted from that of D to obtain donor + acceptor spectra (F_{D+A}). F_{D+A} and F_A were compared to determine the energy transfer efficiency. Spectrum D was an additional control.

RESULTS

Analytical Ultracentrifugation. We quantified associations between all of the participating species, GalR, HU, and O_E−DNA, using equilibrium ultracentrifugation and multiwavelength detection. To test the physiological significance of any physical interactions between HU and GalR, we used both wild-type HU heterodimer and the mutant HUαK18A homodimer. The latter was shown genetically and biochemically to be defective in the proposed HU−GalR interaction in repressosome formation (*14*). The analysis of the multiwavelength absorption data was performed by fitting the data to assumed association models for each of the seven sample cells. Molar concentrations and association constants were estimated as the fitting parameters. The assumed model in each case and the results of the analysis are described below.

GalR. The repressor protein self-associated at low temperatures (<10 °C) to form dimers, which further interacted to give tetramers. No useful data were acquired at temperatures greater than 10 °C since the protein aggregated and no meaningful association model could describe the system. This was likely the result of the duration of the experiment; by the time equilibrium was reached at 14 °C the proteins had been exposed to the centrifugal field for several days. For the lower temperatures, therefore, the mathematical model of the association that best described the data was

$$C_G(r) = C_G(b)\exp[A_G M_G(r^2 - b^2)] + C_G(b)^2\exp[\ln K_{1,2} + 2A_G M_G(r^2 - b^2)] + C_G(b)^4\exp[\ln K_{1,4} + 4A_G M_G(r^2 - b^2)] + e \quad (2)$$

where b is the radius at the cell bottom, M_G = 37086 Da, the molecular mass of the GalR monomer, e is a baseline error which is often present and must be accounted for, and ln $K_{1,2}$ and ln $K_{1,4}$ are the natural logarithms of the equilibrium constants for monomer−dimer and monomer−tetramer interactions, respectively. The equation $A_G = (1 - \bar{v}^o\rho)\omega^2/2RT$ characterizes the centrifugal force, $\bar{v}^o$ being the partial specific volume of the solute and ω being the rotational speed in rad/s. Weighted least-squares fitting of the data with the above mathematical model gives estimates of $C_G(b)$, e, ln $K_{1,2}$, and ln $K_{1,4}$. Figure 1 shows the GalR concentration versus the distance from the meniscus along with the fitted models in the GalR only experiment. The determined natural logarithms of the association constants were ln $K_{1,2}$ = 14.6 and 14.0 and ln $K_{1,4}$ = 41.6 and 39.6 at 2 and 4 °C, respectively. This corresponded to a free energy of association of about 8 kcal/mol for the monomer−dimer association (or K_d = 0.59 μM) and 6.6 kcal/mol for the monomer−tetramer association (or K_d = 6.5 μM).

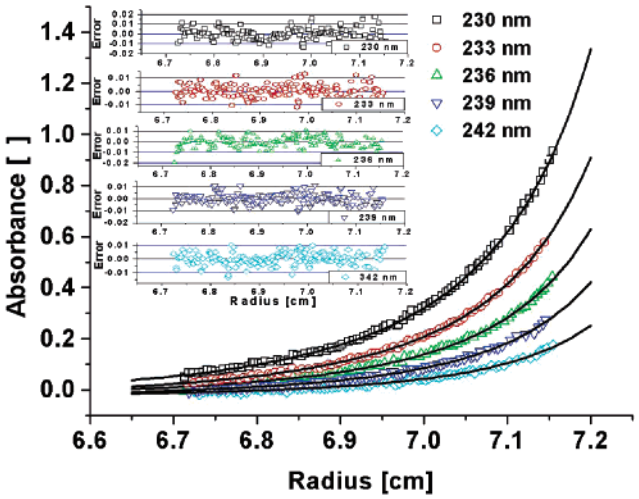

FIGURE 1: Least-squares data fit for multiwavelength absorbance data for a column of GalR alone. Inset graphs show the fitting errors that demonstrate the good quality of the fit. The data were fitted with a model, which expresses the interactions between GalR monomers and dimers and between GalR dimers and tetramers. For clarity, every other point of the complete data set is plotted.

HU. HU heterodimers (HU_2) were found to form weak tetramers themselves, and no higher oligomers were detected even at higher temperatures and after several days in the centrifugal field (Figure 2a). The speed of centrifugation was chosen for the expected species in cells 6 and 7, and it was, therefore, too low for the mass of the HU tetramer. This explains the very shallow gradients seen in Figure 2a. Thus, the confidence intervals were fairly broad (e.g., 99% confidence interval for ln $K_{1,2}$ = 8.3 ± 3.3 at 6 °C). Other models studied include (1) no self-association, (2) HU_2−$(HU_2)_2$−$(HU_2)_4$, and (3) HU_2−$(HU_2)_2$−$(HU_2)_3$. The fitting with models 1 and 3 was unacceptable while the fitting with model 2 was practically identical to that of the monomer−dimer shown in Figure 2a. There was no measurable tetramer present. As HU alone proved to be the most stable of the different systems in the various cells, we were able to collect and analyze data at four different temperatures and five different wavelengths. In addition, the sample that was ran at 24000 rpm and 4 °C gave essentially the same results (K_d = 0.9 mM), and the corresponding data and fit are shown in Figure 2b. This gave us absolute confidence about the stoichiometry and enough confidence about the strength of association. The free energy of association was found to vary between 3.5 kcal/mol (or K_d = 1.7 mM) at low temperatures and up to about 6 kcal/mol (or K_d = 24 μM) at higher temperatures. The mathematical model used here was similar to the one in eq 2. Ultracentrifugation data of HU interactions were analyzed in more detail. The determination of HU tetramerization at four different temperatures (2, 4, 6, and 10 °C) allowed an approximate but informative thermodynamic description of the binding process. The dimer−dimer association seems to be accompanied by significant negative specific heat change (−2 to −2.5 kcal/mol), indicating that the interaction buries many polar groups on the protein surface and is, therefore, driven substantially by hydrophobic bonds. The HUαK18A dimer mutant behaved similarly to the wild type, except that higher oligomers were also detected, although the self-association remained rather weak.

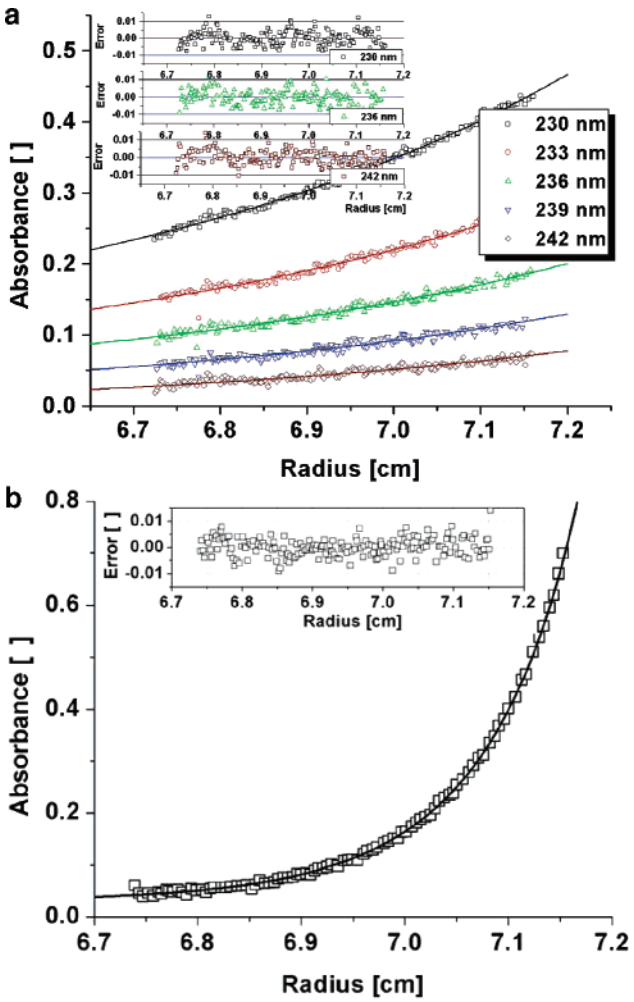

FIGURE 2: (a) Least-squares data fit for multiwavelength absorbance data for a column of HU. Inset graphs show the fitting errors that demonstrate the good quality of the fit. The fitting model describes an equilibrium between HU dimers and tetramers. Data shown were collected at 2 °C and 10000 rpm. (b) Least-squares fit using the same model as in (a) of equilibrium data of wild-type HU at 4 °C and 24000 rpm.

O_E. The O_E−DNA molecule did not show any sign of self-association. Instead, the data were used to compute a more accurate partial specific volume for the molecule than the one obtained from its composition. The data were fit to a single component model as in the first term in eq 2 using $(1 - \rho\bar{v}^o)$ as the fitting parameter. Using the value of the density obtained from densitometer measurements, we computed an accurate value for $\bar{v}^o$ to be 0.4805 at 2 °C for the buffer used. This value was used in the subsequent analysis.

GalR + O_E. For the GalR and O_E−DNA combination, the mean molecular mass in the solution was computed to be about 64 kDa, indicating the presence of a GalR dimer−O_E complex. The interaction model that best fit the data was $2\text{GalR} + O_E \leftrightarrow \text{GalR}_2O_E$. This model gave the best estimates for the natural logarithm of the equilibrium constant for the formation of a GalR_2O_E complex, $\ln K_{\text{GalR}_2O_E} = 30.73$. If it is assumed that the GalR dimers found previously in cell 1 bound one DNA molecule, then the association free energy is fairly strong with free energy of association of about 8.8 kcal/mol (or $K_d = 70$ nM). A similar interaction affinity between GalR and O_E by DNase protection assays was reported previously (*18*).

HU + O_E. In the absence of GalR, HU did not bind to the 20 bp DNA duplex in any detectable measure.

HU + Distorted DNA. We did not measure this interaction by ultracentrifugation. Grove et al. showed a $K_d = \sim 4$ nM as measured by electrophoretic mobility assays (*12*).

HU + GalR. An HU and GalR combination visibly precipitated upon mixing and was not studied.

GalR + HU + O_E. We tested whether HU binds to the GalR dimer−O_E complex observed above and, if so, at what stoichiometry. The question of stoichiometry in the potential GalR dimer−O_E and wild-type HU interaction led us to run two different concentration ratios of GalR and O_E over HU in the two cells. Both cells contained equimolar amounts of O_E and GalR but 1.3- and 1.5-fold higher amounts of HU, respectively. A solution containing the two proteins and the DNA under this condition is expected to contain both monomeric and multimeric species of each of the individual proteins and their different complexes. They include GalR, GalR_2, GalR_4, HU dimer ($\alpha\beta$) and tetramer, O_E, GalR_2−O_E, and the possible ternary complexes of as yet unknown stoichiometry. In all of the corresponding exponential functions, the only unknown parameters were the monomer concentrations while the association coefficients were known from the analysis of the data in cells 1−5. This left the association constant for the formation of the ternary complex as the only other parameter to be estimated. It is known that ultracentrifugation data can be fit well by many such sums of exponentials representing different groups of species. Hence, there is the possibility that more than one model fit the data well. The decision in that case may be based more on the robustness of the fit and the confidence intervals of the estimated parameters rather than on the quality of the fits themselves. The mathematical models for the assumed associations were fit globally to data from both cell 6 and cell 7 at five wavelengths. When a mathematical model containing all of the potential species, in quantities consistent with the association constants estimated from the previous experiments, was fitted to the data, it was clear that additional species were present. The mean molecular mass in the solution was computed to be around 72 kDa, which indicated the possible existence of complexes higher than those found in cell 5 for GalR_2−O_E. As it was already ascertained that a GalR dimer binds to O_E, the models examined included complexes of the GalR_2−O_E with zero to three HU dimers. Clearly, the models with zero and with three HU dimers do not fit the data nearly as well. Both models with one and two dimers, however, fit the data very well. To choose between the two models, we examined the robustness of the least-squares minimization procedure with the two models. In general, the model that included one HU dimer gave a slightly better fitting correlation coefficient (R^2) and slightly better estimation errors, but the differences were not decisive. Figure 3 shows the collected data and the fitted mathematical model along with the residuals of the fits. The fit quality of the data argues strongly in favor of the assumed models with one or two HU dimers, although the exact value of the dissociation constant is limited by the corresponding estimation errors of the association constants for the remaining complexes. The natural logarithm of the molar association constant, $\ln K_{(\text{HU})_2-(\text{GalR})_2-O_E}$, for the formation of the complex was estimated to be 47.3. Since the natural logarithm of the equilibrium constant for the formation of the GalR dimer−

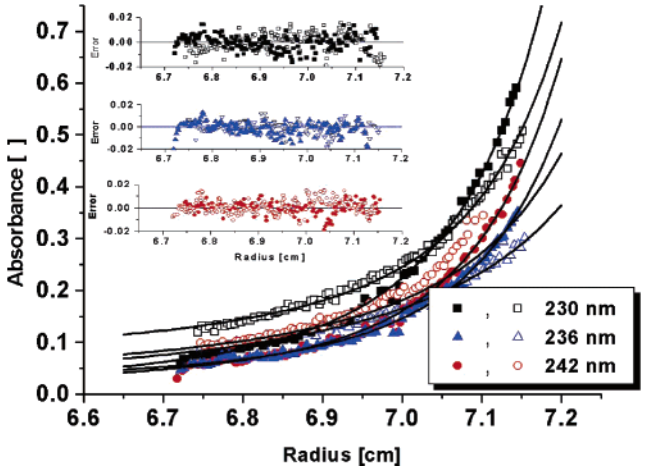

FIGURE 3: Formation of the ternary HU dimer−GalR dimer−O_E complex. Shown are least-squares fits for the multiwavelength absorbance data for two columns containing GalR, HU, and O_E at different excess concentrations of HU. For clarity purposes, only three out of five wavelength data are shown along with the corresponding fitting errors as insets. Every second absorbance data point is shown. Open symbols represent data from cell 6 and closed symbols from cell 7 (see Experimental Procedures). Data for the wavelength of 236 nm was offset for clarity.

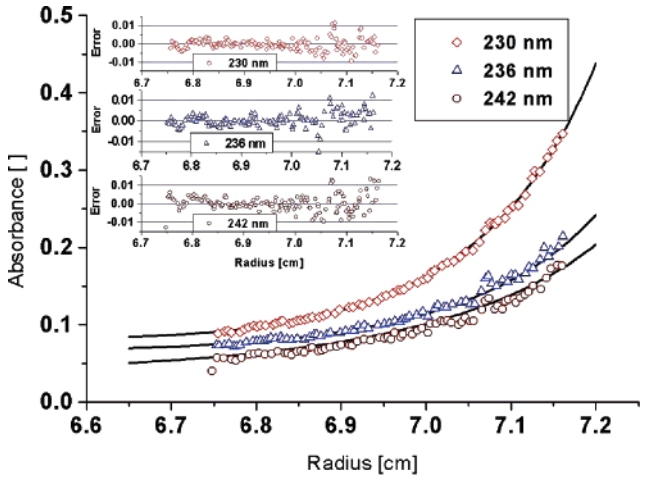

FIGURE 4: Ultracentrifugation data of mutant HU and the GalR dimer−O_E complex. The data fitting for the combined experiment is shown. Although the formation of the ternary complex is included in the model, the least-squares fitting returns a value for the association constant that is zero.

O_E complex was ln $K_{(GalR)_2-(O_E)_1}$ = 30.73, the value of ln K for the binding of the HU dimer to the GalR−dimer−O_E complex was approximately 16.6, which implies a rather strong binding of the HU to the GalR dimer−O_E with free energy of association of about 9.1 kcal/mol (or K_d = 62 nM).

When the mutant HUαK18A dimer was used, the interactions changed significantly. The data, shown in Figure 4, were a better fit with a model that did not include the ternary complex. Using the same association model as with the wild-type HU, the estimated association constant turned out to be effectively zero. This indicated that the mutant form of HU was not capable of binding to the GalR dimer−O_E complex.

Fluorescence Anisotropy. Since the stoichiometry of the HU−GalR interaction was not unambiguously established in the ultracentrifugation experiments, we decided to employ a fluorescence anisotropy technique for this purpose. Fluorescence anisotropy, a direct function of the rotational mobility of the fluorophore, which in turn is a direct function of the size and shape of the molecule, was used to measure protein−protein interactions. Since the mass of a protein increases upon complex formation with another macromolecule, the associated anisotropy increase can be used as a quantitative measure of complex formation (*19*). Wild-type HU does not have any cysteine residue. We employed a mutant HU, HUαA43C/β, with a unique cysteine, to create an attachment point for the fluorescent probes. The HUαA43C/β protein was labeled with IAEDANS as described in Experimental Procedures. The HUαA43C/β and its IAEDANS derivative were shown to be active in repressosome formation (*13*) (data not shown). The AEDANS−HU was titrated with a preformed GalR−O_E complex at an AEDANS−HU concentration (2.5 μM), which is more than 10-fold higher than the dissociation constant obtained by ultracentrifugation. Under these conditions, the tangential lines at zero and infinite concentrations of the GalR−O_E complex cut at the point of stoichiometric equivalence. Figure 5 shows the anisotropy increase of AEDANS−HUαA43C/β as a function of added GalR−O_E complex. The anisotropy increased rapidly and saturated quickly. The tangential lines cut at about 4 μM, which is closer to the 1:1 model than the 2:1 HU−GalR model (in the latter case the intersection point should be at 1.25 μM). Although there is significant scatter in the data, the obtained equivalence point of about 4 μM is the lower limit. Values higher than this would indicate association of more than one GalR dimer with one HU dimer. Although this interpretation is possible from the anisotropy data alone, ultracentrifugation data rule out such a possibility. Thus, combination of ultracentrifugation and fluorescence anisotropy strongly suggests association of one HU dimer with one GalR dimer (bound to O_E). As a control, we performed the same titration in the presence of excess unlabeled HUαA43C/β. There was no significant increase in anisotropy, suggesting a specific interaction between HU and the GalR−DNA complex (data not shown). Taken together with the ultracentrifugation data, the suggested

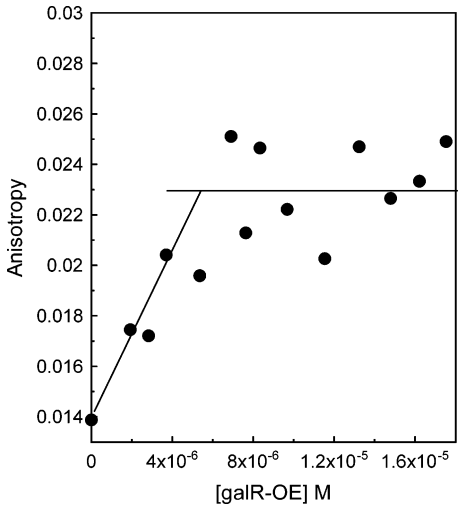

FIGURE 5: Titration of AEDANS−HUαA43C/β with the GalR−O_E complex in 0.1 M Tris-HCl, pH 7.0, and 0.3 M NaCl at 25 °C. The *Y*-axis shows the anisotropy values, which are consistent for a small flexible molecule such as HU. The data points were a combination of two experiments done on two different days. The two lines were drawn to establish the stoichiometric equivalence.

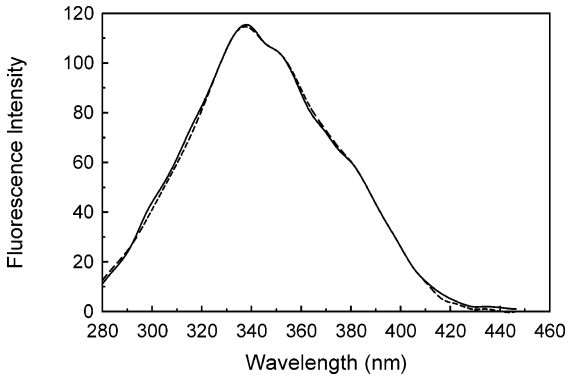

FIGURE 6: Excitation spectra of a solution containing 7.5 μM O_E−DNA, 7.5 μM AEDANS−HUαA43C/β, and 7.5 μM GalR dimer (—) and 7.5 μM O_E−DNA and 7.5 μM AEDANS−HUαA43C/β (- - -). Appropriate controls were subtracted from the spectra shown as described in Experimental Procedures. Emission wavelength was set at 480 nm.

stoichiometry of the HU−GalR interaction is 1:1 (O_E−GalR:HU_2).

Fluorescence Resonance Energy Transfer. Fluorescence energy transfer experiments were carried out between AEDANS−HUαA43C/β and the GalR dimer−O_E complex, at 7.5 μM each, to estimate the magnitude of the distance between HU and GalR−O_E in a ternary complex. This would help us to derive constraints on different association models mentioned in the Discussion. The excitation spectra of solutions containing AEDANS−HUαA43C/β and O_E−DNA and AEDANS−HUαA43C/β, O_E−DNA, and GalR, shown in Figure 6, were virtually identical. No significant difference was seen around 285 nm. If energy transfer occurred from the GalR tryptophan to the AEDANS moiety in HU, higher fluorescence intensity would have occurred at wavelengths where tryptophan absorbs (280−300 nm). On the basis of the intensity values in the observed spectra, we concluded that the energy transfer was very close to zero. The R_0 (where 50% energy transfer occurs) is typically 30−40 Å for the tryptophan−AEDANS pair. Additional uncertainties existed due to κ^2. Even if R_0 is very low (<20 Å), the tryptophan and the AEDANS labels would be at least 40 Å or more away. The energy transfer experiment was also measured between AEDANS−HUαA43C/β and the fluorescein-labeled GalR dimer−O_E complex at concentrations of 3.0 μM each. Although only a partial complex formation is expected at this concentration, no energy transfer was observed by comparison of excitation spectra. Due to high mobility of amino-linked fluorescein at the end of DNA, uncertainty of the value of κ^2 was less in this situation. Typically, R_0 for the AEDANS−fluorescein pair is around 40 Å. After adjustments for relatively low complex formation, we set an upper limit of 50 Å for HU to DNA end distance. Assuming that the donor and acceptor locations in the two energy transfer experiments were oriented correctly, the HU molecule was likely far away from both the DNA ends and the GalR tryptophan in the HU−GalR−O_E complex, suggesting that HU bound not to DNA but to the region of GalR, which is farthest from the DNA.

DISCUSSION

Cooperative binding of HU and GalR to DNA in repressosome formation suggested a protein−protein interaction between HU and GalR (*13*). The interaction model was further supported by the isolation and characterization of HU mutants apparently defective in the proposed interaction (*14*). The fluorescence anisotropy and equilibrium ultracentrifugation experiments presented here confirm a physical association between HU and the GalR−O_E DNA complex. The specificity and biological significance of the ternary complex formation was demonstrated by the fact that the genetically defined, association defective, mutant HU was also incapable of associating with the GalR−O_E complex in the equilibrium ultracentrifugation experiments. These experiments do not completely rule out the possibility that HU interacts with the $GalR_2$−O_E complex not through the $GalR_2$ but through the DNA. However, the fluorescence energy transfer measurements do not support a model in which HU also binds to the 20 bp DNA to which $GalR_2$ binds with high affinity. The existence of the mutant HU, with the mutation farthest from HU's DNA binding motif, which is incapable of ternary complex formation, and fluorescence energy transfer derived constraints argue in favor of direct association of HU and DNA-bound $GalR_2$.

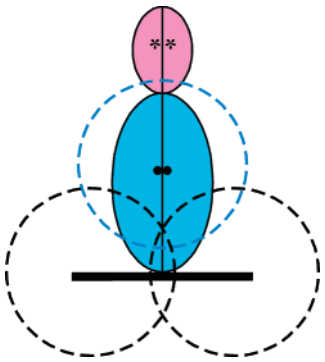

FIGURE 7: A cartoon of the HU dimer−GalR dimer−O_E complex showing the distance limits (not drawn to scale). Key: DNA, solid black rod; GalR, blue ellipsoid; HU, pink ellipsoid. The black bullets in the middle of GalR are the approximate locations of the tryptophan residues in the dimers. The positions of the tryptophans were derived from the homology model of GalR based on the crystal structures of homologous repressors (*30*). The two black dotted circles encompass the 50 Å radii around the ends of DNA fluorescein label, and the blue dotted circle encompasses the 50 Å radius around GalR tryptophan residues. These areas are excluded from the AEDANS labels located approximately in the middle of HU (indicated by stars).

Figure 7 represents a cartoon of different distance limits of HU from $GalR_2$ and DNA obtained from energy transfer measurements. The AEDANS labels, approximately in the middle of the HU structure (indicated by stars), are beyond the 50 Å radii (indicated by black dotted circles) of the two fluorescein-labeled DNA ends and also beyond the 50 Å radius (indicated by a blue dotted circle) of the two tryptophan residues (indicated by black bullets) in the GalR dimer. Energy transfer experiments suggested that the DNA ends and the tryptophan residues in $GalR_2$ are excluded to AEDANS labels in HU, indicating that HU binds to the $GalR_2$−O_E binary complex in the manner shown in the cartoon, i.e., through $GalR_2$. This conclusion is consistent with the lack of complex formation with the HUαK18A homodimer in the ultracentrifugation studies. If HU_2 was binding to the 20 bp DNA duplex directly, and not to $GalR_2$, through its C-terminal DNA binding domain (*20*, *21*), the N-terminal domain where the K18A change is located should

Table 1: Measurement of Association between GalR, HU, and O_E by Equilibrium Ultracentrifugation

interacting molecules	temp (°C)	stoichiometry model	dissociation constant K_d	$\Delta G°$ (kcal/mol)
GalR−GalR	2−10	monomer:dimer	0.59 μM	7.9
	2−10	dimer:tetramer	6.5 μM	6.6
HU−HU (HU = $\alpha\beta$ dimer)	2−14	$\alpha\beta$ dimer:$\alpha\beta$ tetramer	1.7 mM to 24 μM (mean = 0.23 mM)	3.5−6.0 (mean = 4.6)
GalR dimer−O_E	2−10	1:1	76 nM	9.0
HU dimer−GalR dimer−O_E	2−6	1:1:1 or 2:1:1	62 nM or 0.86 μM[a]	9.1 or 6.9[a]
HUαK18A dimer−GalR dimer−O_E	2−6	N/A	>1 M	N/A

[a] For the binding of the dimer of the HU $\alpha\beta$ dimer.

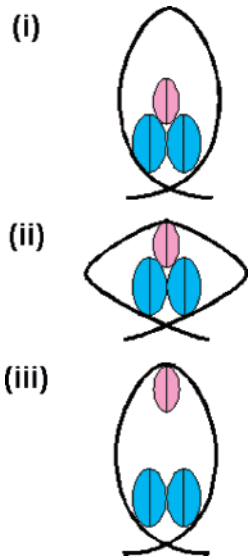

FIGURE 8: Models i−iii of the role of HU in repressosome formation as described in the text. It is assumed that one HU dimer participates in the final structure. Not drawn to scale. The colors of the symbols are as in Figure 7.

not cause any DNA binding defect as was observed in the equilibrium ultracentrifugation results. We have also previously demonstrated that the HUαK18A homodimer is not defective in its general DNA binding property (*14*).

From the energetic parameters of interactions between various components of the Gal repressosome determined in the current study, and the demonstration of specific mutations in HU_2 that disrupt the repressosome formation and at the same time prevent physical interaction with $GalR_2$, it is imperative that the function of HU_2 delineates the pathway of repressosome assembly. On the basis of the observations reported here and previously, we attempted to construe the pathway of repressosome assembly. Because the ability of GalR to tetramerize is weaker than to dimerize (6.6 vs 7.9 kcal/mol; Table 1), the energetic barrier in DNA looping is the required DNA bending and twisting (*22*). Although part of the energetic deficiency is taken care of by supercoiled DNA, HU could help to overcome the energetic barrier, as reported previously, in one of the following three ways in repressosome assembly (*5*) (Figure 8): (i) as a DNA bender to bind to and bend an apical position (*hbs*) in DNA, (ii) as an adapter to facilitate tetramerization of GalR, or (iii) as both to establish permanent contact with $GalR_2$ while remaining DNA (*hbs*) bound. In an adapter role (model ii), HU_2 keeps the GalR tetramer together and, thus, stabilizes the DNA bend without DNA contact. The demonstration of GalR tetramer formation by ultracentrifugation studies (Table 1), the ability of mutant GalR proteins to interact with each other in the absence of HU using a genetically defined

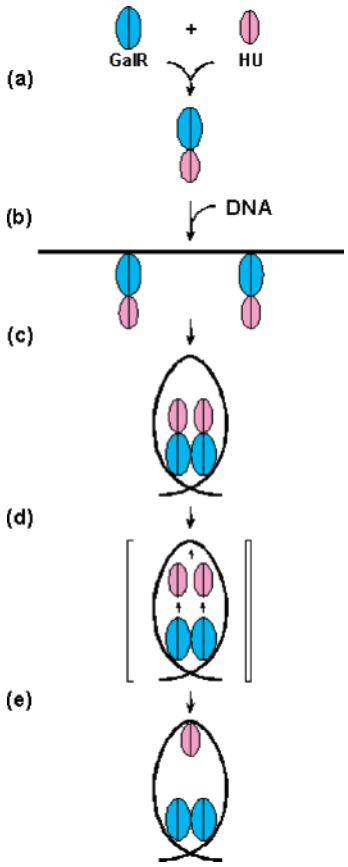

FIGURE 9: A pathway of Gal repressosome formation (steps a−e). The colors of the symbols are as in Figure 7. The details are discussed in the text. The intermediate stage between steps d and e has not been demonstrated and is shown within the bracket.

interface (*23*), and the existence of a specific HU−DNA contact between the two operators in repressosome formation (*13*) rule out a simple adapter model. Given the limited size of the DNA segment (113 bp), a DNA loop-containing structure with simultaneous contacts between two GalR molecules and an HU molecule and the three proteins simultaneously contacting their cognate DNA (model iii) would be energetically and/or sterically prohibitive (*22*). Consistent with model i, the atomic force microscopic observations suggested that the Gal repressosome does not have any contact between GalR and HU (unpublished results).

We, therefore, propose the following pathway for building the model i structure (Figure 9): (a) GalR dimers recruit HU. (b) GalR−HU complexes bind to the operators. (Step b could precede step a.) (c) The operator-bound GalR−HU complexes transiently interact to form tetramers and generate a DNA loop that has a distortion around the apical region. (d) Spontaneous dissociation of HU from GalR increases the

local concentration of HU. (e) The dissociated HU binds to the transiently bent/distorted DNA, stabilizing the structure of model i. This pathway is consistent with the energetics of the various interactions reported above. In this scenario, HU plays an architectural role in Gal repressosome formation. GalR piggybacks HU for delivery to the transiently bent/distorted DNA bent and thus overcomes the entropic barrier. The concentration of HU in the cell is not high enough to interact with a rare and transient target in *gal* DNA. The recruitment of HU by GalR as a piggyback in Gal repressosome formation to overcome an entropic barrier may be an example of a common theme in the formation of similar higher order structures involving both architectural and sequence-specific DNA binding proteins in other DNA transaction reactions (*24*−*29*).

ACKNOWLEDGMENT

We thank Drs. Dhruba Chattoraj and Susan Garges for critically reading the manuscript.

REFERENCES

1. Adhya, S. (1989) Multipartite genetic control elements: communication by DNA loop, *Annu. Rev. Genet. 23*, 227−250.
2. Schleif, R. (1992) DNA looping, *Annu. Rev. Biochem. 61*, 199−223.
3. Choy, H. E., Park, S. W., Aki, T., Parrack, P., Fujita, N., Ishihama, A., and Adhya, S. (1995) Repression and activation of transcription by Gal and Lac repressors: involvement of alpha subunit of RNA polymerase, *EMBO J. 14*, 4523−4529.
4. Irani, M., Orosz, L., and Adhya, S. (1983) A control element within a structural gene: the gal operon of *Escherichia coli*, *Cell 32*, 783−788.
5. Aki, T., Choy, H. E., and Adhya, S. (1996) Histone-like protein HU as a specific transcriptional regulator: co-factor role in repression of gal transcription by GAL repressor, *Genes Cells 1*, 179−188.
6. Adhya, S., Geanacopoulos, M., Lewis, D. E., Roy, S., and Aki, T. (1998) Transcription regulation by repressosome and by RNA polymerase contact, *Cold Spring Harbor Symp. Quant. Biol. 63*, 1−9.
7. von Wilcken-Bergmann, B., and Muller-Hill, B. (1982) Sequence of galR gene indicates a common evolutionary origin of lac and gal repressor in *Escherichia coli*, *Proc. Natl. Acad. Sci. U.S.A. 79*, 2427−2431.
8. Bianchi, M. E. (1994) Prokaryotic HU and eukaryotic HMG1: a kinked relationship, *Mol. Microbiol. 14*, 1−5.
9. Bonnefoy, E., Takahashi, M., and Rouvière-Yaniv, J. (1994) DNA-binding parameters of the HU protein of *Escherichia coli* to cruciform DNA, *J. Mol. Biol. 242*, 1116−1129.
10. Castaing, B., Zelwer, C., Laval, J., and Boiteux, S. (1995) HU protein of *Escherichia coli* binds specifically to DNA that contains single-strand breaks or gaps, *J. Biol. Chem. 270*, 10291−10296.
11. Kobryn, K., Lavoie, B., and Chaconas, G. (1999) Supercoiling-dependent site-specific binding of HU to naked Mu DNA, *J. Mol. Biol. 289*, 777−784.
12. Grove, A., Galeone, A., Mayol, L., and Geiduschek, E. P. (1996) On the connection between inherent DNA flexure and preferred binding of hydroxymethyluracil-containing DNA by the type II DNA-binding protein TF1, *J. Mol. Biol. 260*, 196−206.
13. Aki, T., and Adhya, S. (1997) Repressor induced site-specific binding of HU for transcriptional regulation, *EMBO J. 16*, 3666−3674.
14. Kar, S., and Adhya, S. (2001) Recruitment of HU by piggyback: a special role of GalR in repressosome assembly, *Genes Dev. 15*, 2273−2281.
15. Majumdar, A., Rudikoff, S., and Adhya, S. (1987) Purification and properties of Gal repressor:pL-galR fusion in pKC31 plasmid vector, *J. Biol. Chem. 262*, 2326−2331.
16. Lewis, M. S., Shrager, R. I., and Kim, S.-J. (1994) Analysis of protein-nucleic acid and protein-protein interactions using multi-wavelength scans from the XL-A analytical ultracentrifuge, in *Modern Analytical Ultracentrifugation* (Shuster, T. M., and Laue, T. M., Eds.) pp 94−115, Birkhauser, Boston.
17. Bandyopadhyay, S., Deb, S., Bose, S., and Roy, S. (2002) Half-of-the-sites reactivity of F235C lambda-repressor: implications for the structure of the whole repressor, *Protein Eng. 15*, 393−401.
18. Brenowitz, M., Jamison, E., Majumdar, A., and Adhya, S. (1990) Interaction of the *Escherichia coli* Gal repressor protein with its DNA operators in vitro, *Biochemistry 29*, 3374−3383.
19. Lakowicz, J. R. (1999) *Principles of Fluorescence Spectroscopy*, 2nd ed., p 309, Plenum Publishing Corp., New York.
20. White, S. A., and Draper, D. E. (1989) Effects of single-base bulges on intercalator binding to small RNA and DNA hairpins and a ribosomal RNA fragment, *Biochemistry 28*, 1892−1897.
21. Rice, P. A., Yang, S., Mizuuchi, K., and Nash, H. A. (1996) Crystal structure of an IHF-DNA complex: a protein-induced DNA U-turn, *Cell 87*, 1295−1306.
22. Geanacopoulos, M., Vasmatzis, G., Zhurkin, V. B., and Adhya, S. (2001) Gal repressosome contains an antiparallel DNA loop, *Nat. Struct. Biol. 8*, 432−436.
23. Semsey, S., Geanacopoulos, M., Lewis, D. E., and Adhya, S. (2002) Operator-bound GalR dimers close DNA loops by direct interaction: tetramerization and inducer binding, *EMBO J. 21*, 4349−4356.
24. Nash, H. A. (1996) The *E. coli* HU and IHF proteins: accessory factors for complex protein-DNA assemblies, in *Regulation of Gene Expression in E. coli* (Lin, E. C. C., and Lynch, A. S., Eds.) pp 149−179, R. G. Landes Co., Georgetown, TX.
25. Echols, H. (1990) Nucleoprotein structures initiating DNA replication, transcription, and site-specific recombination, *J. Biol. Chem. 265*, 14697−14700.
26. Santero, E., Hoover, T. R., North, A. K., Berger, D. K., Porter, S. C., and Kustu, S. (1992) Role of integration host factor in stimulating transcription from the sigma 54-dependent nifH promoter, *J. Mol. Biol. 227*, 602−620.
27. Wassem, R., De Souza, E. M., Yates, M. G., Pedrosa, F. D., and Buck, M. (2000) Two roles for integration host factor at an enhancer-dependent nifA promoter, *Mol. Microbiol. 35*, 756−764.
28. Thomas, J. O., and Travers, A. A. (2001) HMG1 and 2, and related "architectural" DNA-binding proteins, *Trends Biochem. Sci. 26*, 167−174.
29. De Beer, T., Fang, J., Ortega, M., Yang, Q., Maes, L., Duffy, C., Berton, N., Sippy, J., Overduin, M., Feisss, M., and Catalano, C. E. (2002) Insights into specific DNA recognition during the assembly of a viral genome packaging machine, *Mol. Cell 9*, 981−991.
30. Geanacopoulos, M., Vasmatzis, G., Lewis, D. E. A., Roy, S., Lee, B. K., and Adhya, S. (1999) GalR mutants defective in repressosome formation, *Genes Dev. 13*, 1251−1262.

BI047720T